Measuring Woody Encroachment along a Forest-Savanna Boundary in Central Africa

Measuring Woody Encroachment along a Forest–Savanna Boundary in Central Africa

E. T. A. Mitchard*

School of Geosciences, University of Edinburgh, Edinburgh, United Kingdom

S. S. Saatchi

Jet Propulsion Laboratory, California Institute of Technology, Pasadena, California

F. F. Gerard

Centre for Ecology and Hydrology, Wallingford, United Kingdom

S. L. Lewis

Earth and Biosphere Institute, School of Geography, University of Leeds, Leeds, United Kingdom

P. Meir

School of Geosciences, University of Edinburgh, Edinburgh, United Kingdom

Received 14 August 2008; accepted 20 May 2009

ABSTRACT: Changes in net area of tropical forest are the sum of several processes: deforestation, regeneration of previously deforested areas, and the changing spatial location of the forest–savanna boundary. The authors conducted a long-term (1986–2006) quantification of vegetation change in a 5400 km^2

* Corresponding author address: E. T. A. Mitchard, Institute of Geography, School of Geosciences, University of Edinburgh, Drummond St, Edinburgh, EH8 9XP, UK.
E-mail address: edward.mitchard@ed.ac.uk

DOI: 10.1175/2009EI278.1

forest–savanna boundary area in central Cameroon. A cross-calibrated normalized difference vegetation index (NDVI) change detection method was used to compare three high-resolution images from 1986, 2000, and 2006. The canopy dimensions and locations of over 1000 trees in the study area were measured, and a very strong relationship between canopy area index (CAI) and NDVI was found. Across 5400 km^2 12.6% of the area showed significant positive change in canopy cover from 1986 to 2000 (0.9% yr^{-1}) and 7.8% from 2000 to 2006 (1.29% yr^{-1}), whereas <0.4% of the image showed a significant decrease in either period. The largest changes were in the lower canopy cover classes: the area with <0.2 m^2 m^{-2} CAI decreased by 43% in 20 years. One cause may be a recent reduction in fire frequency, as documented by Along Track Scanning Radiometer-2/Advanced ATSR (ATSR-2/AATSR) data on fire frequency over the study area from 1996 to 2006. The authors suggest this is due to a reduction in human pressure caused by urbanization, as rainfall did not alter significantly over the study period. An alternative hypothesis is that increasing atmospheric CO_2 concentrations are altering the competitive balance between grasses and trees. These data add to a growing weight of evidence that forest encroachment into savanna is an important process, occurring in forest–savanna boundary regions across tropical Africa.

KEYWORDS: Woody encroachment; Ecotone; Change detection

1. Introduction

It has long been appreciated that the woody cover of large areas of tropical Africa has undergone rapid changes in the recent past, with forest having retreated to a small fraction of its present area because of an arid period from circa 4000 to 1300 years before present, and having expanded to its present extent by around 900 years before present despite increasing human pressure (Maley 1996; Salzmann and Hoelzmann 2005). Many factors interact to control the woody cover of an area, including rainfall, soil characteristics, seasonality, temperature, and the level and history of disturbance (Sankaran et al. 2005; Bucini and Hanan 2007). The majority of the woody savannas of Africa would, in the absence of disturbance, become forest: Sankaran et al. (Sankaran et al. 2005) show that if mean annual precipitation (MAP) is greater than 650 mm, then only disturbance (fire, herbivory, timber extraction) prevents canopy closure. This has been confirmed by the observation of rapid woody encroachment in long-term fire exclusion experiments in Ghana (Swaine et al. 1992), Burkina Faso (Menaut 1977), and Ivory Coast (Vauttoux 1976).

Assessing the dynamics of the tropical forest–savanna boundary is important, as change will have large influences on people, ecosystems, and human populations. Changes in tree cover in the wide ecotone between rain forest and dry savannas in Africa depend on the relative strengths of many processes, the most important of which are forest clearance for agriculture and pasture, forest degradation for timber and fuel, changes in fire frequency, and climate change (which includes increasing atmospheric CO_2 concentrations, increasing air temperature, and changes in precipitation; Malhi and Wright 2004). Climate change excepted, increased human presence increases the first three of these, reducing the tree cover of an area, whereas reduced human impact will result in a reduction in these factors, and both an expansion of forest into savannas and a general increase in the woody cover of

those savannas (Bucini and Hanan 2007). The importance of fire frequency cannot be overstated here: almost all fires in African savannas are anthropogenic in origin, and given the ability of fires to spread widely from where they are set they have the potential to influence the vegetation across large areas, even far from human settlements (Favier et al. 2004). The impact of anthropogenic climate change on these ecosystems is still uncertain: although increasing temperatures are likely to reduce the competitiveness of trees over C4 grasses, increasing CO_2 concentrations do the reverse, reducing the advantage C4 grasses have over C3 trees (Lloyd and Farquhar 2008). Increased atmospheric CO_2 concentrations have also been hypothesized to lead to increased success of trees in savannas because of a reduced transpiration rate leading to increased water percolation and reduced seedling mortality (Polley et al. 1997), and by increasing the ability of saplings to resprout successfully following fire damage, thus making it more likely that they will escape the flame zone (Bond and Midgley 2000). While it is appreciated that increased rainfall would over the long term increase tree cover, provided the effect is not negated by increasing temperature (Hély et al. 2006), significant uncertainties exist as to the long-term precipitation trends in the region (Bernstein et al. 2007). These uncertainties are exacerbated by the fact that changes in vegetation in this sensitive region will result in strong feedbacks with climate (Zeng and Neelin 2000).

There is a large body of evidence that woody encroachment (involving both trees and shrubs) into semiarid savannas and grasslands is occurring (Archer et al. 2001; Eamus and Palmer 2007); Archer et al. (Archer et al. 2001) found 28 studies showing increases in woody vegetation in Africa and 202 studies finding such changes worldwide. There are fewer studies finding such an increase in tropical savannas, but some do exist: for example in northern Australia (Hopkins et al. 1996; Bowman et al. 2001; Russell-Smith et al. 2004; Brook and Bowman 2006), the Western Ghats of India (Puyravaud et al. 2003), and South America (Duarte et al. 2006; Durigan and Ratter 2006; Marimon et al. 2006; Roitman et al. 2008). In Africa just four studies showing increasing tree cover in tropical rain forest–savanna boundary regions have been reported. Boulvert (Boulvert 1990) drew on anecdotal evidence to suggest that woody expansion was occurring in the forest–savanna ecotones of central Africa because of the urbanization of the population but provided little concrete evidence. Happi (Happi 1998) compared a high-resolution aerial photograph from 1950 with Landsat thematic mapper (TM) data from 1990 to find gallery forest encroachment into surrounding savannas at a rate of 0.6–2 m yr^{-1} in central Cameroon. Guillet et al. (Guillet et al. 2001) used field studies and soil carbon isotopes ($^{13}C/^{12}C$, ^{14}C) along two transects in eastern Cameroon to show both significant expansion of the forest and that increased woody cover of the savanna has occurred over the past century. Nangendo et al. (Nangendo et al. 2005) used a combination of field studies and vegetation index–based satellite change detection to find a 14% increase in woody vegetation over a 14-yr period in the woodlands of the Budongo Forest Reserve, Uganda. However, all the African studies are small in scale and reliant on detailed local field data for success, and as such their methods are not easily applicable to a larger spatial scale, which is necessary to assess whether this forest encroachment is indeed widespread. No studies showing the opposite process, woody regression, were found for Africa apart from in areas where there has been an increase in anthropogenic activity, for example, around cities and in areas of agricultural encroachment.

Mapping woody cover from remote sensing data can follow a wide range of different methods. Manual interpretation is best suited to hyperspatial satellite data and aerial photographs (Couteron et al. 2001; Xiao and Moody 2005). Classification-based methodologies can be effective (Sedano et al. 2005; Su et al. 2007), but the imposition of artificial classes can result in a tendency toward subjectivity and lead to an overestimation of dominant classes and underestimation of rare classes (e.g., Couteron et al. 2001) and was thought especially unsuitable for this study as finding changes in woody cover within a class (e.g., woody savanna) is not possible. Empirical regressions between vegetation indices or red reflectance can be successful, often finding very strong relationships (Leprieur et al. 2000; Lu et al. 2003; Ferreira et al. 2004; Ferreira and Huete 2004), though problems of soil reflectance (Chen et al. 1998; Leprieur et al. 2000) and the influence of the herbaceous vegetation (Fuller et al. 1997; Qin and Gerstl 2000) must be considered. More sophisticated techniques that can consider more bands—for example, spectral mixture analysis or neural networks, or metrics that include image texture in addition to spectral information—are becoming increasingly accepted; they are, however, very sensitive to differing environmental conditions, sensor type and calibration, solar-target geometry, and atmospheric conditions, and as such are not appropriate for change detection unless there are good ground data for all dates (Coppin et al. 2004; Lu et al. 2004; Lu 2006).

Numerous techniques have been developed for bitemporal change detection, but they can be broadly classed into three categories: postclassification comparisons, image differencing/ratioing, and more sophisticated multiband algorithms (such as change vector analysis or cross-calibration analysis) (Coppin et al. 2004; Lu et al. 2004). Which methodology is chosen depends on the environment being analyzed and the types of data being used: remotely sensed or ground data. In general, when changes in clear categories of land cover are being assessed, classification-based methodologies are appropriate; where the variable being assessed is relatively simple and different sensors or exact atmospheric correction is not possible, image differencing is preferred; and where identical sensors are used and good atmospheric and field data are available, more sophisticated change algorithms may be appropriate, though in most cases they do not give superior results to image differencing–based methodologies (Coppin et al. 2004).

In this paper we examine changes in woody cover in a large study area in central Cameroon. The normalized difference vegetation index (NDVI) derived from Landsat and Advanced Spaceborne Thermal Emission and Reflection Radiometer (ASTER) remote sensing platforms is used in combination with field studies, coarse spatial resolution data [Advanced Very High Resolution Radiometer (AVHRR)], and very high spatial resolution satellite imagery (Quickbird) to identify and characterize with great confidence the changes in woody cover from 1986 to 2006. The methods presented here, because of their relative simplicity and the ready availability of historical NDVI data, allow the possibility of scaling up to a regional level using coarser-resolution data.

2. Study area

The study area is a 5400 km^2 region in central Cameroon, centered on 6°1′22″N, 12°48′40″E, and encompasses the northern two-thirds of the Mbam Djerem

National Park and the area to the north of the park, including the town of Tibati and Lake Mbakauo. This region was chosen as it includes a complete range of regional vegetation types, from forest in the south contiguous with the Congo basin rain forest belt, through a forest–savanna matrix in the north of the park, to savanna with narrow gallery forests in the north of the study area (see Figure 1). It experiences an annual rainfall of 1650 mm, with a pronounced dry season (average 4 mm $month^{-1}$) from December to March [Climatic Research Unit (CRU) TS 2.1 dataset (Mitchell and Jones 2005) and Tropical Rainfall Measuring Mission (TRMM) 3B43 V6 satellite data (Kummerow et al. 2001)]. The human population of the southern part of the study area is very small and has decreased over the study period because of the formation first of the Reserve de Faune de Pangar et Djerem in 1982, which encompasses 2400 km^2, and then the Mbam Djerem National Park in 2000, which expanded this to 4165 km^2. The population density in the northern half of the study area is higher but still low, with the only major population center being the town of Tibati, which has increased in population by almost 90% over the study period, from 15 522 in the 1987 census to an estimated 28 981 by 2007 (CIESIN 2004). Small-scale agriculture occurs around settlements, and there is a limited amount of nomadic cattle herding passing through the area; local people believe this has decreased significantly over the past 20–30 years. Significant levels of fishing occur within the park, though there are attempts to reduce this (Ministère des Forêts et de la Faune 2007), and also occur in all the rivers and lakes in the study area.

3. Methods

3.1. Field data

The study area was visited October–December 2007 as part of the Tropical Biomes in Transition field campaign (TROBIT; www.geog.leeds.ac.uk/groups/trobit/). Eight transects 20 m wide and 100–200 m long were set up and positioned in three different areas near the Djerem River in the north to middle of the Mbam Djerem National Park (see Figure 1). Seven of these transects ran from forest to savanna, with one entirely in forest. All trees with a diameter at 1.3 m [diameter at breast height (DBH)] greater than 5 cm had their diameter, height, canopy dimensions (distance from trunk to outermost leaf measured for all four compass points), and species identity recorded. A total of 1009 trees, representing 79 species from 33 families, were measured (see appendix A for species list). Each tree was located using a handheld differential GPS (Trimble GeoHX, Trimble, United States); these positions were later corrected using data from the Scripps Orbit and Permanent Array Center (SOPAC) N'Koltang ground station in Libreville, Gabon, using the H-Star differential correction facility in the software GPS Pathfinder Office 3.10 (Trimble, United States), resulting in accuracies of <0.5 m in the horizontal direction and <1 m in the vertical dimension. The transects were divided into 30-m sections, and the canopy dimensions used to calculate the vertically projected canopy area for each region of the transects (an elliptic canopy shape was assumed), which we named the canopy area index (CAI). The changes in species composition in the different portions of the eight transects are detailed in appendix A.

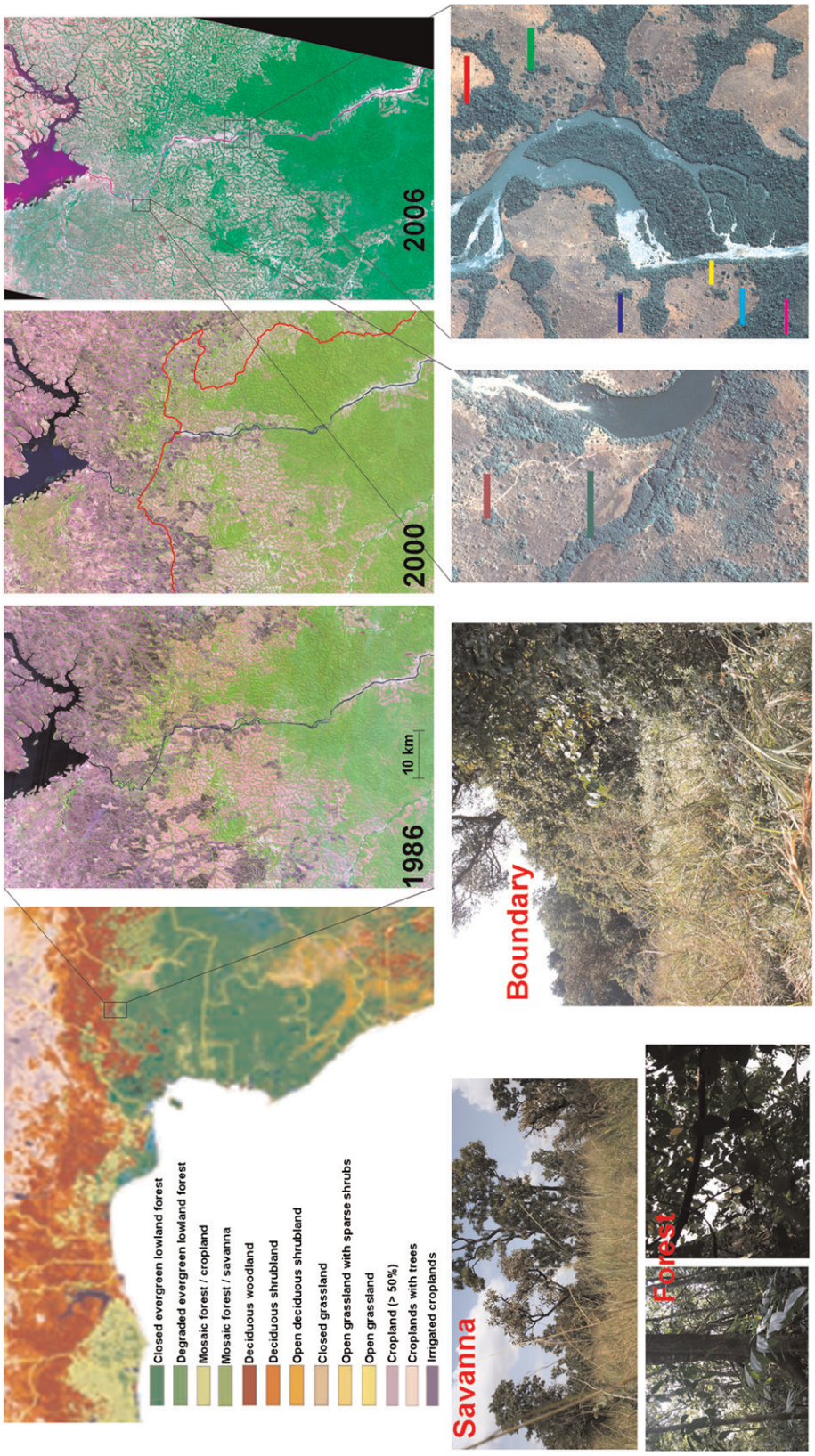
2006
2000
1986
10 km
Closed evergreen lowland forest
Degraded evergreen lowland forest
Mosaic forest / cropland
Mosaic forest / savanna
Deciduous woodland
Deciduous shrubland
Open deciduous shrubland
Closed grassland
Open grassland with sparse shrubs
Open grassland
Cropland (> 50%)
Croplands with trees
Irrigated croplands
Boundary
Savanna
Forest

3.2. Remote sensing data

A Landsat TM image captured on 30 December 1986 and a Landsat Enhanced TM Plus (ETM+) image captured on 12 December 2000, both for path 156 row 56, were downloaded from the Global Land Cover Facility. Both were provided at a pixel size of 28.5 m. Two ASTER scenes, between them covering almost the whole study area, captured 4 December 2006, were acquired from the National Aeronautics and Space Administration (NASA) Land Processes Distributed Active Archive Center. Of the ASTER scene only the visible and near-infrared bands were used in further analysis, which were provided at a 15-m pixel size. Two 0.6-m-resolution Quickbird images were acquired from Eurimage covering all the field sites, by a combination of a 12 × 8 km archive image from 19 February 2004 covering the northern field sites, and a 10 × 10 km new acquisition, captured 23 January 2008, covering the southern field sites.

To remove atmospheric effects from the TM, ETM+, and ASTER data, atmospheric correction was performed using atmospheric/topographic correction software package (ATCOR)-2 (ReSe, Switzerland). This model used the post-launch offsets and gains and a tropical atmospheric model to produce reflectance images. The software package ENVI (ITT, United States) was used for all subsequent remote sensing analysis. The two ASTER scenes were mosaicked together, and visual analysis of the join showed it to be seamless. No sharp changes in the reflectance values of any bands were apparent in 20 transects placed across the join of the two images, so no further correction of the individual scenes was considered necessary. This outcome was expected given that the scenes were captured with the same sensor within 10 s of each other.

The 60 × 90 km study area was subsetted from the 2000 ETM+ image, and the 1986 TM image was georeferenced to this using a network of 40 visually selected ground control points taken from features such as road junctions, islands, small clumps of trees, and branching points of gallery forests, with a resulting root-mean-square error (RMSE) of 0.37 pixels (10.5 m). Similarly the 2006 ASTER mosaic was georeferenced to the 2000 ETM+ image, with a network of 38 ground control points resulting in an RMSE of 0.35 pixels (10 m). The ASTER image was subsequently resampled to 28.5-m pixels using the pixel aggregate method.

Given the difficulties of calibrating images captured by different sensors under different unknown atmospheric conditions, we decided to analyze the changes using normalized univariate image differencing, implemented on cross-calibrated

←

Figure 1. (top row) Vegetation map taken from Mayaux et al. (Mayaux et al. 2004) showing the location of the study area within Cameroon, with the three satellite images compared in this study: Landsat TM from 1986, Landsat ETM+ from 2000, and ASTER mosaic from 2006. The north and east borders of the Mbam Djerem National Park are shown in red on the 2000 image. (bottom row) Pictures taken from the study area in 2007, showing typical forest and savanna biomes, as well as the sharp transition between the two; portions of Quickbird images showing the location of the eight transects where canopy cover was measured.

vegetation indices. Univariate image differencing essentially subtracts one date of imagery from another date and is often chosen as the preferred change detection approach for tropical environments (Coppin et al. 2004; Lu et al. 2004), with Coppin et al. (Coppin et al. 2004) stating in their conclusions summary that "image differencing and linear transformations appear to perform generally better than other bitemporal change detection methods." More sophisticated change detection techniques were thought to be unsuitable for this analysis, as the sensor used at each time point is different, and absolute atmospheric correction of the earlier scenes is not possible.

Using vegetation indices, which are in effect a ratio between two spectral bands, reduces the errors inherent in univariate change detection analyses because ratios between bands are affected to a smaller degree by different atmospheric conditions and different sensor characteristics than raw reflectance values (Coppin et al. 2004; Pettorelli et al. 2005). These indices are developed from the red and near-infrared bands, and their response to vegetation cover is widely acknowledged (e.g., Huete et al. 2002). The visible red wavelengths are absorbed by chlorophyll in vegetation, and near-infrared wavelengths are strongly reflected by the plant cuticle and cell wall, giving higher values for vegetation than for nonvegetated surfaces. As all three images were captured in the early dry season, when the grass layer is dead and dry, containing no chlorophyll, but leaves are still present on most trees, it is to be expected that the value of a vegetation index in a pixel will correspond directly to the CAI of that pixel (Fuller et al. 1997; Qin and Gerstl 2000; Archibald and Scholes 2007). Vegetation indices have been shown to be strongly related to woody cover in savanna environments on a number of occasions (e.g., Lu et al. 2003; Ferreira et al. 2004; Ferreira and Huete 2004). Typical problems with using these indices, such as topography and soil reflectance, were minimized in this study as the study area has little relief and is not large enough to have much heterogeneity in the CAI to vegetation index relationship.

We investigated the use of three vegetation indices: the NDVI, the modified soil adjusted vegetation index (MSAVI) (Qi et al. 1994), and the enhanced vegetation index (EVI) (Huete et al. 1994). The EVI, though it appeared to be very sensitive to vegetation and as such was good for comparing the two Landsat scenes, was abandoned because of the necessity of a blue band (450–515 nm), which is not present in ASTER data. MSAVI, designed to minimize the influence of soil reflectance, produced a small dynamic range for this ecosystem, and though it did differentiate forest from savanna well, it was less successful than NDVI. NDVI was therefore the vegetation index chosen for all subsequent analysis. Its formula is

$$\mathrm{NDVI} = \frac{b_n - b_r}{b_n + b_r}, \tag{1}$$

where b_n is the near-infrared band (750–900 nm) and b_r is the red band (630–690 nm).

The NDVIs from the 1986 TM and 2006 ASTER images were then calibrated to the 2000 ETM+ image using linear regression models derived from 25 known invariant targets (i.e., their land-cover type and appearance did not change in any of the three images). These targets were drawn from water bodies, grasslands, and dense tropical forest [1986–2000, $\mathrm{NDVI}_{\mathrm{adj}} = -0.1804 + 0.9009(\mathrm{NDVI}_{86})$,

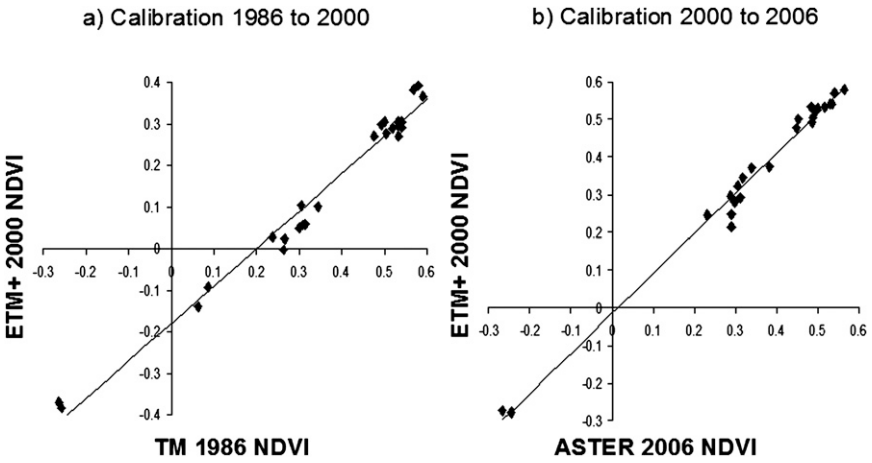

Figure 2. NDVI cross-calibration points, drawn from suspected unchanged areas such as water bodies, grasslands, and dense tropical forest, plotted for (a) ETM+ 2000 against TM 1986 and (b) ETM+ 2000 against ASTER 2006.

$r^2 = 0.98$; 2006–00, $\text{NDVI}_{\text{adj}} = -0.0226 + 1.069(\text{NDVI}_{06})$, $r^2 = 0.98$, see Figure 2]. This process should have removed most remaining calibration problems between the different sensors and atmospheres, and it is as successful as absolute radiative correction (Songh et al. 2001; Coppin et al. 2004), which is not possible here because of the lack of accurate atmospheric data for the 1986 image.

To test that NDVI is correlated with woody cover, the NDVI values extracted from the ASTER 2006 pixels covering each 30-m section of the eight transects were regressed against the CAI measured in situ (defined as m^2 canopy divided by m^2 ground area). A different georeferencing was used here, involving two 10×10 km sections taken from the 15-m adjusted-NDVI ASTER image and performing a very detailed tie-point matching process with the ground control point-corrected Quickbird data (which is estimated to be geocorrected to <2 m). RMSE values were always less than 0.3 ASTER pixels (<4.5 m), based on at least 50 tie points, so it is possible to be very confident that the NDVI values extracted correspond to the portions of the transects measured on the ground.

To examine whether precipitation was similar during November–December 1986, 2000, and 2006, a combination of the weather station and modeling-derived CRU TS 2.1 dataset (1901–2002; Mitchell and Jones 2005) and the TRMM Microwave Imager (TMI) 3B43 V6 satellite data (1998–2007; Kummerow et al. 2001) were used to estimate the rainfall in these months. The monthly precipitation data at a 0.5° resolution were used in both cases, making these two data sources readily comparable. These datasets were also analyzed for long-term rainfall and temperature trends over the study area (1901–2007).

To confirm that trends observed at individual time slices are representative of a genuine trend and not merely caused by problems with calibration or different environmental conditions, NDVI values from the Global Inventory Modeling and Mapping Studies (GIMMS) AVHRR 8-km dataset (Pinzon et al. 2005; Tucker et al. 2005) were extracted over the study area. These data were examined for trends in

the annual average NDVI as well as the annual average NDVIs for the dry and wet seasons.

As fire frequency is considered an important factor in controlling woody cover, an estimate of the changes in fire frequency over the study area was also desirable. No data of sufficient sensitivity exist for the whole study period (AVHRR fire data detected just six hot spots in the study area from 1986 to 2006), so data were acquired from the Along Track Scanning Radiometer-2 and Advanced ATSR (ATSR-2/AATSR) World Fire Atlas from 1996 to 2006. Fires detected from within the study area were extracted and the number of fires counted for each year. This thermal anomaly dataset is known to be accurate, having very good geolocation and low commission errors (Arino et al. 2005; George et al. 2006), but it is also acknowledged that it underestimates the total fire number because of both a lack of sensitivity to low-intensity fires and the nighttime detection missing daytime fires. However, this is not of concern here, as we are interested in the trend in fire frequency, not the absolute rate of fire occurrence.

3.3. Change detection

Image comparisons were performed between 1986 and 2000 and 2000 and 2006. However, before any comparisons, water bodies and urban areas were masked from all images by excluding any pixels with a negative NDVI. A proportion of savanna areas were clearly burn scars and found to have an NDVI between 0.05 and 0.16. Leaving these areas in the analysis with their raw NDVI values would bias the analysis, as the same area changing from burnt grassland to unburnt grassland would appear to have increased in woody cover, whereas in fact no change would have occurred. Rather than exclude these areas from the analysis, which would reduce the area available to detect changes, the value of all unmasked pixels with an NDVI < 0.2 was adjusted to 0.2. This in effect converted all the burnt areas in the images to areas with the same NDVI as savanna with a CAI of 0–0.2 $m^2\ m^{-2}$, as it is assumed that areas that burn in this way, early in the dry season, will have a low CAI (Lambin et al. 2003; Felderhof and Gillieson 2006). The validity of this procedure was confirmed by the observation that the majority of burnt patches in the 1986 image have similar NDVI values to their surrounding, unburnt, areas after this procedure is applied. To confirm that this procedure is not driving the observed results, an identical analysis was performed without this process, instead using a supervised classification to remove all the burnt areas (see appendix B).

Rather than comparing the simple differences in NDVI between the various time points [as recommended by Singh (Singh 1989) and used by, e.g., Nangendo et al. (Nangendo et al. 2005)], we decided to normalize the changes by comparing the difference ratioed by the sum of the pixels, as this further increases confidence in the results of vegetation index differencing change detection (Coppin et al. 2004). This is because difference values of the same absolute magnitude vary in significance depending on the size of the original NDVI values: an increase from 0.25 to 0.35 is much more significant than an increase from 0.45 to 0.55 (see Figure 3), but a simple differencing method will predict the same magnitude of change for both. The formula used for the change detection was, therefore,

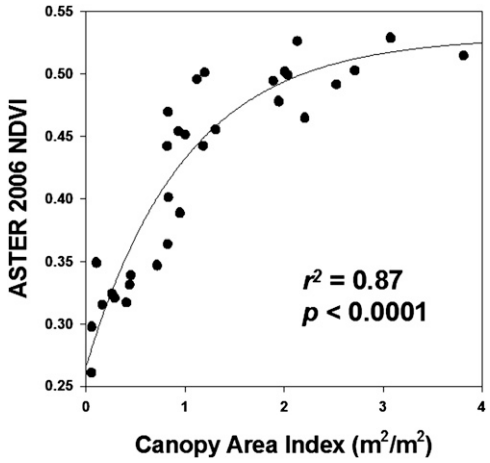

Figure 3. Adjusted ASTER 2006 NDVI regressed against field-measured CAI (m^2 canopy per m^2 area) for 30-m sections of field transects.

$$\text{Change} = \frac{\text{NDVI}_{\text{new}} - \text{NDVI}_{\text{old}}}{\text{NDVI}_{\text{new}} + \text{NDVI}_{\text{old}}}. \tag{2}$$

This produces change images, with every pixel having a value from -1 to $+1$, where zero indicates no change, positive values positive change (i.e., an increase in woody cover), and negative values negative change (i.e., a decrease in woody cover). The resulting distribution of points was tested for normality using a Shapiro–Wilk normality test, and then the standard deviation of the distribution was calculated, allowing an assessment of how much of a deviation from zero indicates a significant change in woody cover. The pixels were therefore grouped into classes according to the number of standard deviations each pixel deviated from zero, with $<\pm$ one standard deviation considered no change, $>\pm$ one standard deviation considered marginally significant change, and $>\pm$ two standard deviations considered significant change at approximately the 95% confidence level.

The tight relationship between the in situ measured CAI and ASTER NDVI makes it possible to look at absolute changes in the extent of woody cover over the study area. To do this the relationship between NDVI and projected CAI was applied to the NDVI image in each of the three time points, and the ground area in five cover classes quantified (water bodies, urban areas, and areas not present in the 2006 mosaic were not included).

4. Results

4.1. Sensitivity of NDVI to CAI

NDVI is shown to be strongly correlated with field-measured CAI (m^2 m^{-2}) in this environment ($r^2 = 0.87$, $p < 0.0001$, $n = 32$; see Figure 3). CAI is directly

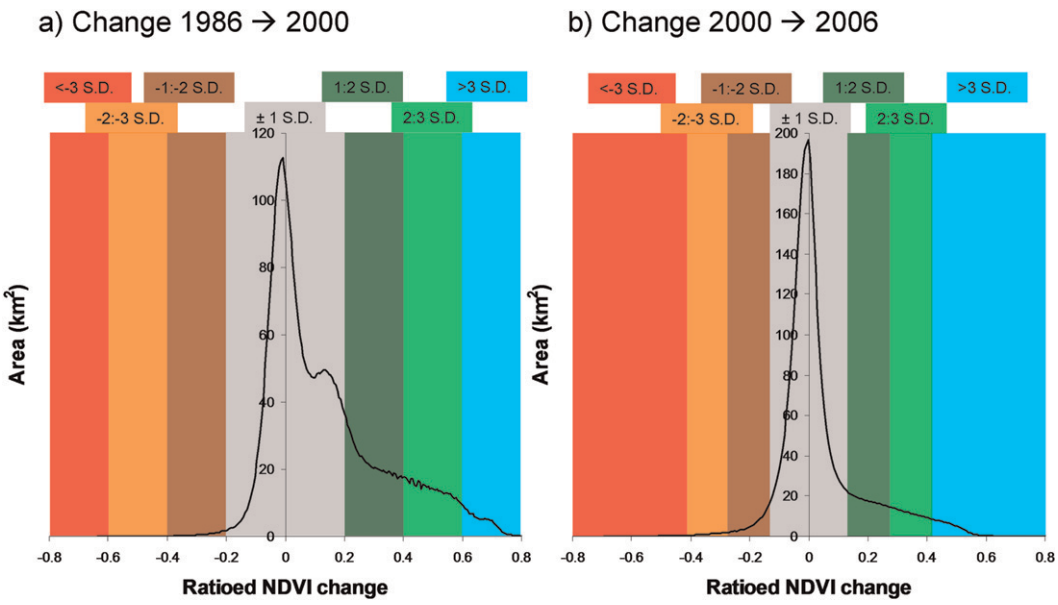

Figure 4. Histograms showing the area covered by pixels in each 0.05 range of ratioed NDVI change, for the 1986–2000 and 2000–06 analyses. Standard deviations of the distribution are overlaid, with colors corresponding to those used in Figure 5.

proportional to the density and size of trees per unit area and believed therefore to be a good measure of woody cover. The fitted line is

$$\mathrm{NDVI} = 0.27 + 0.26(1 - e^{-\mathrm{CAI}}), \tag{3}$$

which can be rearranged to

$$\mathrm{CAI} = -\ln\left(\frac{0.53 - \mathrm{NDVI}}{0.26}\right). \tag{4}$$

Sensitivity decreases rapidly above a CAI of 2 $\mathrm{m}^2\ \mathrm{m}^{-2}$, but NDVI is undoubtedly a very good metric for detecting changes in the woodiness of savannas and the position of the forest–savanna boundary, giving confidence that the change detection shown below relates to genuine changes in woody vegetation.

4.2. Change detection

Both normalized image differencing analyses produced normal distributions centered on 0, with a positive skew, suggesting, respectively, that the cross-calibration process was effective and that increases in NDVI were observed

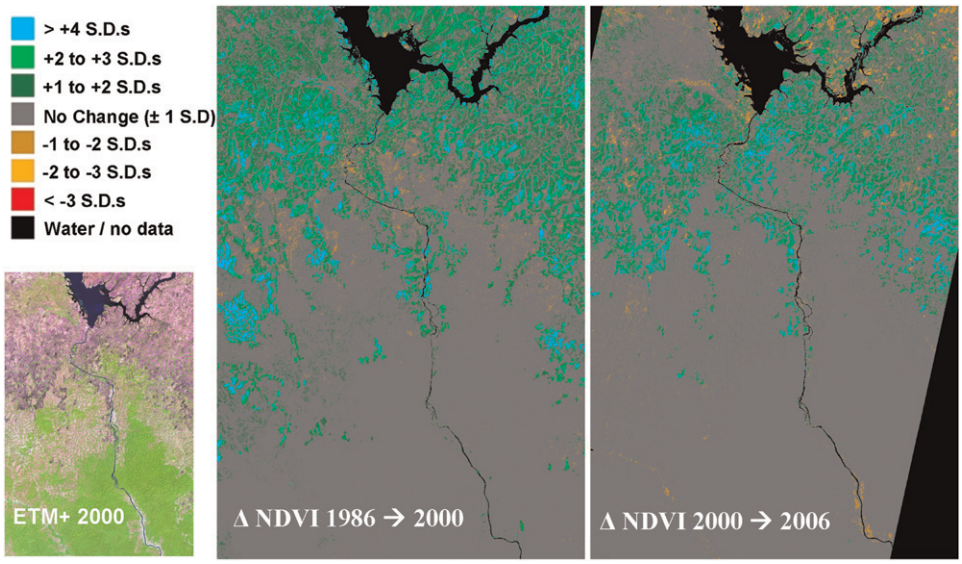

Figure 5. Two images showing the change in NDVI between 1986 and 2000 and 2000 and 2006, in standard deviations (see text). Changes >± two standard deviations should be considered significant at the 95% level. The 5–4–3 composite image from 2000 is also included to show that the increases in NDVI occurred in the savannas, consistent with an increase in woody vegetation.

(Figure 4). When thresholded according to standard deviations, very significant increases in NDVI over savanna regions are found both between 1986 and 2000 and 2000 and 2006, as displayed in Figure 5 and Table 1. A significant positive increase in NDVI (> two standard deviations, approximately equivalent to a 95% confidence level) can be seen in 12.57% of the study area from 1986 to 2000 and 7.76% from 2000 to 2006. There is evidence from this that the rate of woody encroachment has risen over the 20-yr period, as the percentage increase divided by the number of years of comparison is 0.9% yr^{-1} from 1986 to 2000 but 1.29% yr^{-1} from 2000 to 2006. In contrast, the number of pixels showing significant negative trends is negligible in both comparisons.

Applying Equation (4) to the NDVI images allowed an assessment of how the area covered by each vegetation type has changed over the study period. The results of this are displayed in Figure 6. While less sensitive than the change detection analysis, because of inaccuracies in the CAI–NDVI relationship and the necessity to categorize the vegetation into distinct classes, this analysis is useful in that it can quantify which cover classes experienced the most rapid change. This showed that the largest changes are occurring in the low CAI classes, with the area of grassland (less than 0.2 m^2 CAI per m^2 ground) decreasing by 43% over the 20 years, from 2132 km^2 in 1986 to 1214 km^2 in 2006. All the other classes increase over the study period, with the largest increase in the 0.2–0.4 m^2 m^{-2} CAI class and the smallest in the >1 m^2 m^{-2} CAI class.

Table 1. Percentage and area of change images falling into each change class in the two comparisons, TM 1986 with ETM+ 2000 and ETM+ 2000 with ASTER 2006. The percentage significant positive change divided by the number of years of comparison is also included.

Class	1986–2000		2000–06	
	Percent	Area (km^2)	Percent	Area (km^2)
Significant positive change (>+2 std dev)	12.57	679.2	7.76	419.1
Marginally significant positive change (>+1 std dev)	12.46	673	8.02	433
No change (−1 to +1 std dev)	70.28	3795.1	73.35	3960.7
Marginally significant negative change (<−1 std dev)	1.32	71.2	1.68	90.7
Significant negative change (<−2 std dev)	0.08	4.3	0.38	20.4
Masked (water/urban areas/areas not present in 2006 mosaic)	3.28	177.1	8.82	476.0
Significant positive change per year (%)	0.9% yr^{-1}		1.29% yr^{-1}	

Similar trends were found in the analysis where burnt areas where removed prior to the change analysis (see appendix B). The trends found were approximately half the magnitude of the changes above, as would be expected given the large areas of savanna that were removed; however, this provides evidence that the above results are not an artifact of the thresholding methodology used to enable to inclusion of burnt areas.

4.3. High temporal resolution NDVI record

The AVHRR GIMMS NDVI record shows no significant trend in the annual average or the wet-season average from 1982 to 2006. However, there is a very clear increasing trend in the dry-season NDVI (see Figure 7), showing that the trends found in the high spatial but low temporal resolution dry-season analysis are part of a larger trend.

4.4. Rainfall, temperature, and fire frequency

No significant long-term trends were found in the rainfall or temperature data for the study site. Average annual temperature fluctuated from just 22.5° to 23.6°C, with no obvious trends and, while annual rainfall was more variable, most of the variation was due to fluctuations in the wettest months, and still no trends were apparent (see Figure 8). For the above remote sensing–based change detection to be valid it is essential that precipitation in the months preceding the image capture are identical, otherwise the results could be due to changes in the greenness of the vegetation (especially grasses) not to changes in CAI. A comparison was made of precipitation in the month of image capture, 3 months before image capture, and 6 months before image capture; no differences are apparent between years in the month of image capture or the average of the previous 3 months (see Figure 9). However, there does appear to have been greater average rainfall in 2006 than in the other 2 years when the 6-month average is compared. This should not interfere with the results as the grass layer should still have been dead in 2006; however, it

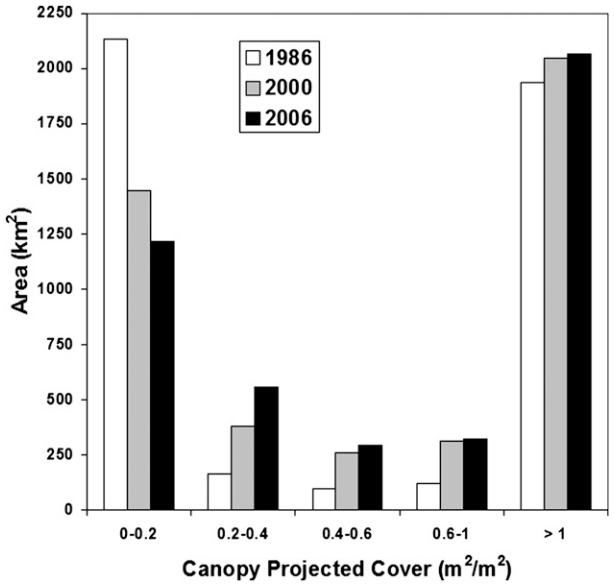

Figure 6. Changes in the total area of vegetation found in different CAI classes in 1986, 2000, and 2006.

should be considered when interpreting the results of the second period of change detection.

Analysis of the ATSR-2/AATSR data provides some evidence that fire occurrence in the study area decreased over the second half of the study period (from 1996 to the present); unfortunately, there are no suitable data for the first half, as AVHRR data have too coarse a resolution and are not sufficiently sensitive to detect these small-scale fires. Figure 10 displays the result, with linear regression finding a significant negative trend in fire frequency against time (gradient $= -1.08$ fires per year, $r^2 = 0.57$, $p < 0.01$, $n = 11$).

5. Discussion

5.1. Woody encroachment

Woody encroachment is occurring rapidly in the Mbam Djerem National Park, corroborating smaller-scale (40–600 km^2) studies showing woody expansion in the forest–savanna ecotones of Africa. This also confirms observations within the study area in November 2007, where forest edges were dominated by young pioneer trees, with dead and dying savanna trees prevalent, which is strong evidence that this constituted young encroaching forests (E. T. A. Mitchard and S. L. Lewis 2007, personal observation; and also the presence of savanna trees in the forest sections of all transects; see appendix A). When looking at the change maps, it is possible to see changes along some gallery forests, suggesting they have increased in width. However, the resolution of the comparisons, 28.5 m, means that even

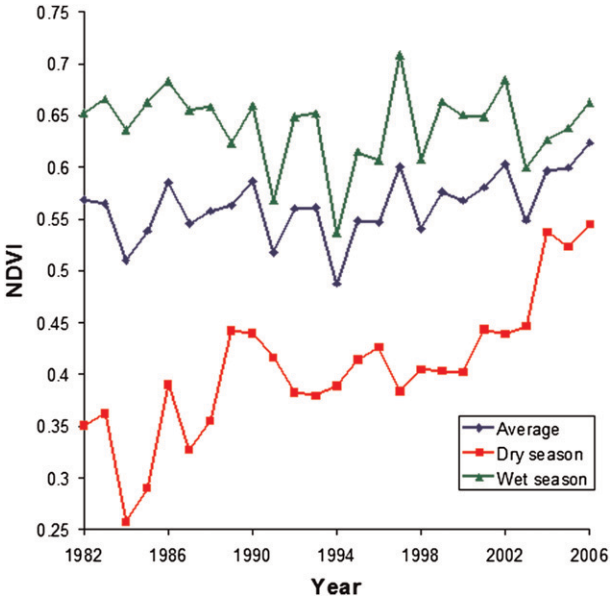

Figure 7. Trends in AVHRR average NDVI for the study area derived from GIMMS data (Pinzon et al. 2005; Tucker et al. 2005). Red points show the average dry-season NDVI (December–March), green points the average wet-season NDVI (April–November), and blue the annual average NDVI.

relatively rapid increases in the size of forests are unlikely to be detected by this method: the forest advance rate of 2 m yr^{-1} found in a nearby region by Happi (Happi 1998) would equate to a movement of 28 m (one pixel) in the 1986–2000 comparison, and 12 m (under half a pixel) in the 2000–06 comparison, both of which could be missed because of slight inaccuracies in the georeferencing. The majority of the increases detected are thus an increase in the woodiness of the savannas, rather than an increase in forest area, as can be seen in Figure 6. We note that, though we are confident the changes we observe genuinely represent an increase in woody cover, the lack of historical field data and local rainfall data prevents us from rejecting the possibility that some or all of these changes are artifacts caused by increases in dry-season rainfall causing greener grasses. We believe the data presented in Figures 7–9 show that this is unlikely to be the case, but without historical field data we cannot be entirely certain, especially for the second period of change detection (2000–06), where, though the rainfall for the preceding 3 months is similar to that in the other 2 years, the preceding wet season had higher rainfall (though it is possible this could be an artifact of using TRMM data, which appears to produce much more variable results in the wet season than the CRU 2.1 dataset; see Figure 8).

While the legal formation of the Mbam Djerem National Park is responsible for some of this gain, slightly over half of the significant positive change in both comparisons occurred outside the park. The likely cause of these changes is hard to determine with confidence, but local people considered the changes due to reductions in human population density, caused by urbanization, resulting in

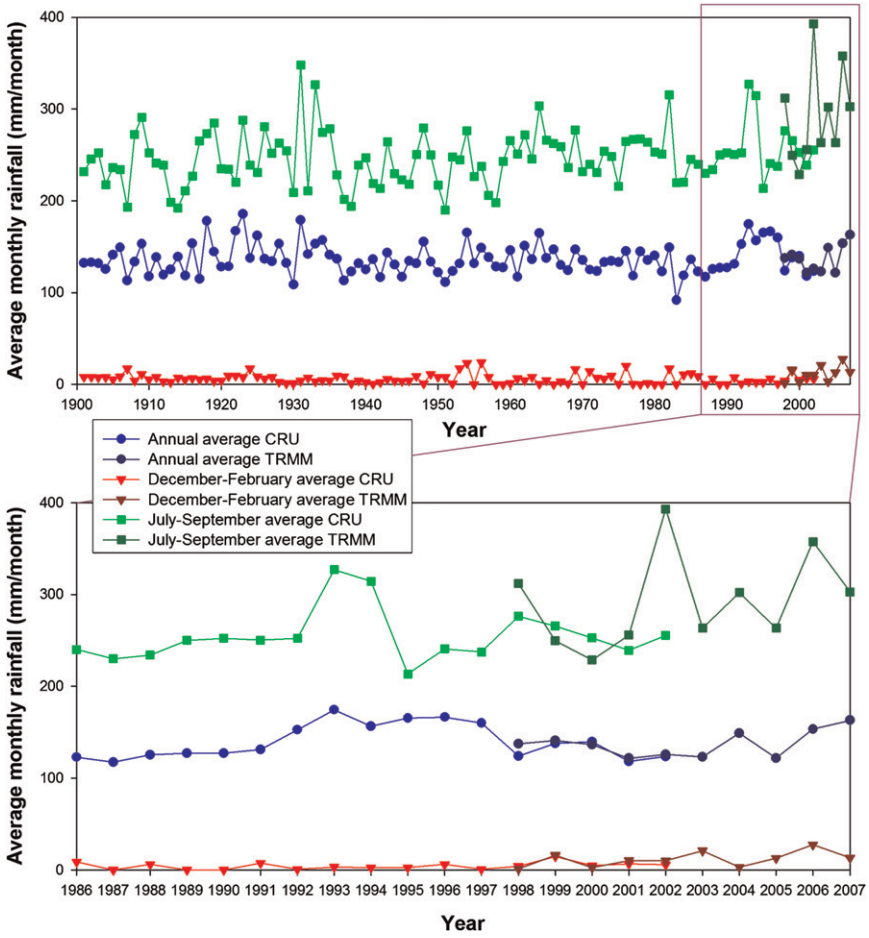

Figure 8. Rainfall data for the study area from 1901 to 2007, showing the average annual rainfall (mm month^{-1}), average rainfall in the driest 3 months (December–February, with December taken from the previous year), and average rainfall in the wettest 3 months (July–September). The data shown are CRU 2.1 modeled/measured data (1901–2002) and TRMM 3B43 V6 satellite data (1998–2007). The study period is also shown in more detail.

decreased burning of the savannas and thus an increase in the number and size of trees (E. T. A. Mitchard and S. L. Lewis 2007, personal communication). They also observe that nomadic cattle herding has moved to other more profitable areas, so burning to produce a flush of grass for cattle is also less widespread. The establishment of the Chad–Cameroon Petroleum Development and Pipeline Project by the World Bank in 2000 may also be an important factor. This project brought the prospect of jobs and consequently caused a shift in the labor force from the mid-1990s (Guyer 2002). The Mbam Djerem National Park also owes its creation in 2000 to this project, which was initially funded by the World Bank with the aim of offsetting some of the environmental damage caused by the project. There is a low-frequency trend distinguishable in the increase in

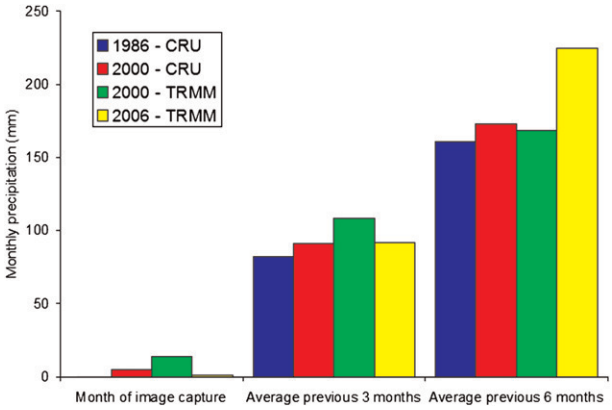

Figure 9. Monthly rainfall over the study site for the month of image capture—average of 3 previous months and average of previous 6 months—for 1986, 2000, and 2006. For 1986 the data are derived from the CRU 2.1 dataset, for 2000 from both the CRU 2.1 and TRMM 3B43 V6 data, and for 2006 only TRMM data.

dry-season GIMMS NDVI data (Figure 7), with rapid increases in the 1980s and 2000s, but a stagnation in the 1990s. The increase from 2000 is easy to explain as it coincides both with the creation of the Mbam Djerem National Park and the Chad–Cameroon Pipeline, as discussed above. The change in the 1980s may be concurrent with urbanization and a reduction in cattle herding, though it is harder to explain why this increase disappears in the 1990s without better local demographic data.

Our analysis of the ATSR-2/AATSR World Fire Map data for the study area from 1996 to 2006 goes some way toward confirming the reduction in fire activity in the area, putatively caused by a reduction in human impact. Although this satellite sensor is not able to detect low-intensity fires, which represent the majority of fires in the study area, the data are unbiased and as such general trends are thought likely to correspond to genuine changes in fire frequency in an area (Arino et al. 2005). The approximate halving in fire frequency over a 10-yr period we see here therefore provides some evidence that a reduction in fire frequency has occurred. Unfortunately, it is impossible to know what the fire frequency was in the mid-1980s over this area as the only satellite data available are not sensitive enough to detect the small-scale fires typical of this ecosystem, but we hypothesize that it was considerably higher than present.

There are no reliable population data available at a sufficient resolution to ascertain whether population levels have genuinely fallen in the study area over the time period considered here. Data for the whole of Cameroon show that, while the urban population has risen at an average 4.44% yr^{-1} from 1986 to 2006, rural population has only increased by only 0.69% yr^{-1} over the same period (World Bank 2007). It is therefore possible that the rural population could have fallen in this small area, as local people suggest, especially given that the population density is already very low (excluding the towns of Tibati and Yoko, the Global

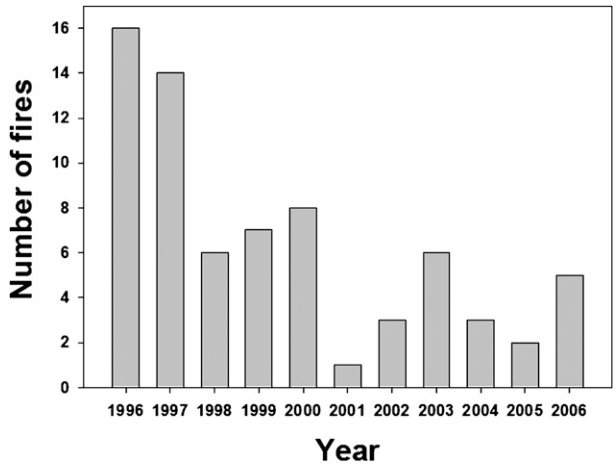

Figure 10. Annual fire count for the study area from 1996 to 2006 derived from ATSR-2 and AATSR World Fire Atlas, using the more sensitive algorithm 2.

Rural–Urban Mapping Project estimates the population density of the area to be just two people per square kilometer; CIESIN 2004).

Analysis of the rainfall and temperature data suggests that this woody encroachment is not environmentally driven. However, it is possible that part of the increase could be due to slight increases in average rainfall. In particular the years 1992–97 stand out as 6 consecutive years where the average annual rainfall is consistently above the long-term average (Figure 8). There is no increase in the average dry-season rainfall during this period, however, where an increase in rainfall would be most likely to influence the survival of woody vegetation both through reduced water stress and a reduction in fire intensity and area (Hély et al. 2006), and equally this increase in precipitation occurs in a period where no increase in dry-season NDVI is detected in the coarse-resolution GIMMS dataset (Figure 7). It has also been suggested that, while rainfall may not have increased, there is evidence of a global reduction in pan evaporation, putatively caused by decreased wind speed and decreased receipt of solar radiation due to increased cloud cover and atmospheric aerosol content (Eamus and Palmer 2007). Such a reduction would have the same effect as an increase in rainfall, increasing soil moisture, which in combination with the potential reduction in stomatal conductance caused by an increase in the CO_2 concentration (Lloyd and Farquhar 2008) could explain woody encroachment. Though Eamus and Palmer's (Eamus and Palmer 2007) model is more suited to arid and semiarid systems than the more mesic environment studied here, the intense dry season makes this a possible causal factor.

5.2. Potential of methodology

The finding that NDVI is very well correlated with CAI in forest–savanna ecotones opens a realm of possibilities for change detection and monitoring of

tropical woody vegetation. NDVI can be calculated from numerous sensors at a full range of resolutions and is easily available in products such as the GIMMS AVHRR data, which has global coverage at an 8-km resolution from 1982 to the present. In this study the trend of increasing CAI detected at a high resolution is clearly matched by an increase in NDVI in the dry-season GIMMS dataset. This provides potential for using dry-season coarse-resolution NDVI data to examine changes both at a continental scale [e.g., using AVHRR or Moderate Resolution Imaging Spectroradiometer (MODIS)] to assess large-scale changes in woody vegetation, and at a more localized scale (e.g., using Landsat and ASTER), for example, to monitor the success of avoided deforestation or carbon sequestration forestry projects. However, heterogeneity of climate and soil may introduce difficulties when using this methodology at a larger scale, though these could potentially be overcome with good ground truthing and potentially further reduced by analysis of the annual NDVI cycle made possible by the daily revisits of coarser-resolution satellite sensors. It is clear that such data must always be analyzed with reference to a precipitation dataset.

Acknowledgments. The authors wish to thank two anonymous reviewers for their detailed comments on an earlier draft of the manuscript. Gatsby Plants for provided ETAM's Ph.D. studentship, and TROBIT, a NERC-funded consortium, Grant NE/D005590/1, funded the rest of the fieldwork. SLL is funded by a Royal Society Research Fellowship; PM is funded by a Royal Society of Edinburgh Research Fellowship. Jon Lloyd, TROBIT P.I., provided useful advice and expertise. Jeanette Sonké, Wildlife Conservation Society-Cameroon (WCS-Cameroon), the University of Yaounde I, and 14 canoeists from Mbakaou provided invaluable support in Cameroon. Adam Freedman provided useful advice on the sources of accurate population data, and Thijs vanden Bergh helped collate the fire data. Remote sensing data were provided by the USGS Global Landcover Facility (Landsat and ASTER), Eurimage (Quickbird), ESA ATSR World Fire Atlas (ATSR-2/AATSR hot spot data), and the NASA Giovanni Rainfall Archive (TRMM rainfall data). The CRU TS 2.1 dataset was downloaded from the University of East Anglia's Climate Research Unit at www.cru.uea.ac.uk/~timm/grid/CRU_TS_2_1.html.

Appendix A

The Locations of Tree Species Found

This is a complete list of tree species found in the eight transects. The species are divided into forest and savanna species, based on knowledge of the ecology of the species in question. Each of the eight transects are divided into three sections according to their average CAI: savanna (CAI < 0.5), transitional forest (CAI 0.5–1), and forest (CAI > 1). Transect 4 did not contain a savanna portion. Note the presence of 24 individuals of savanna species in the forest sections of the transects (all old trees, all but one of which had a DBH > 20 cm), compared with just three individuals of forest species found in the savanna (all of which were young trees with a DBH < 10 cm). These data support the hypothesis that forest is expanding into savanna.

Appendix A.

			Savanna							Transition								Forest							
		Transect number	1	2	3	5	6	7	8	1	2	3	4	5	6	7	8	1	2	3	4	5	6	7	8
Species type	Family	Species																							
Savanna tree	Annonaceae	*Annona senegalensis*	6	4		19																			
	Araliaceae	*Cussonia arborea*				1			2								3								
	Arecaceae	*Borassus aethiopum*			4			2								1									2
	Bombacaceae	*Ceiba pentandra*														1									
	Celastraceae	*Maytenus senegalensis*	7					2	3																
	Combretaceae	*Combretum molle*	2	3	5	1						1					2								
		Terminalia albida		1	7	16	23								2					1			1		
		Terminalia avicennioides			4																				
		Terminalia indet					9								4										
		Terminalia macroptera	11	4		1				4	4			1				1							
		Terminalia schimperiana						1																	
	Euphorbiaceae	*Bridelia ferruginea*	7		2						1							1	1						
		Bridelia speciosa		1							1														
		Hymenocardia acida	9	6	23	47	15	13	2	1	2	2	2	8	10	1					2	2	1		
		Maprounea africana							2																
		Maprounea membranacea	4			2								1											
		Phyllanthus muellerianus							1																
	Fabaceae	*Entada africana*		2		2		12								1									
		Piliostigma indet					10								3								3		
		Piliostigma reticulatum			7							1													
		Piliostigma thonningii	12	10				1	3	1							5	1	1						
	Hypericaceae	*Psorospermum febrifugum*				2																			
	Meliaceae	*Trichilia emetica*	1	2		8			1	1	1										1	1			
	Moraceae	*Ficus abutilifolia*				1																			
		Ficus exasperata	2														1								
		Ficus mucuso																			1				
		Ficus sycomorus			2											2								1	
	Myrtaceae	*Syzygium guineense*	12		2												3								

APPENDIX A. (*Continued*)

			Savanna							Transition								Forest							
		Transect number	1	2	3	5	6	7	8	1	2	3	4	5	6	7	8	1	2	3	4	5	6	7	8
	Ochnaceae	*Lophira lanceolata*	7			5			1					1			1									
		Ochna schweinfurthiana				2																				
	Proteaceae	*Protea madiensis*	2																							
	Rubiaceae	*Crossopteryx febrifuga*	9	1		23		5	10					4			2					1				
		Nauclea indet			1																					
		Sarcocephalus latifolia	3	2					2				1			1						1				1
	Simaroubaceae	*Quassia undulata*							1																	
Forest tree	Anacardiaceae	*Sorindeia indet*																1			16					
		Spondias indet																		1	8					
		Spondias mombin											2								3		10			
	Annonaceae	*Xylopia aethiopica*									1		2	4					4		6	8	1			2
	Apocynaceae	*Funtumia africana*																					1			
		Funtumia elastica											2	1							10	5				
	Bignoniaceae	*Markhamia tomentosa*																2	1							
	Boraginaceae	*Cordia africana*																							1	
	Chrysobalanaceae	*Parinari indet*																			1					
	Clusiaceae	*Garcinia indet*																								4
	Ebenaceae	*Diospyros zenkeri*																			2					
	Euphorbiaceae	*Bridelia indet*																	2							
		Margaritaria discoidea														1				1					1	1
		Uapaca guineense									2	1		1					18	10	2	2		19	6
	Fabaceae	*Afzelia africana*															1									
		Albizia zygia				1				2				1		2		1	1							
		Aphanocalyx djumaensis																			1					
		Berlinia grandiflora																			2				9	
		Daniellia oliveri															6									2
		Detarium macrocarpum																				4				3
		Erythrophleum ivorense												1								4	1			
		Parkia biglobosa																			1				4	

Flacourtiaceae	*Oncoba dentata*					1							12						
	Oncoba indet										1		1				1		
	Oncoba spinosa																2		
Hypericaceae	*Harungana madagascariensis*									1			4						
Irvingiaceae	*Klainedoxa gabonensis*												1						
Lauraceae	*Beilschmiedia indet*												2						
Meliaceae	*Khaya ivorensis*												1						
	Khaya senagalensis																1		
Moraceae	*Ficus indet*									2									
Myristicaceae	*Pycnanthus angolensis*													4	1				
Ochnaceae	*Ochna afzelii*			1	2	1	3	2			2		11	21	3				
Olacaceae	*Olax subscorpioidea*								3						1				
Phyllanthaceae	*Antidesma laciniatum*						4						4		8		1		
	Antidesma membranaceum					5							11						
	Antidesma venosum	1															1		
Sapindaceae	*Allophylus africanus*			4	1		1		1		3	2	1		9		5		
Sterculiaceae	*Cola lateritia*														1				
	Cola laurifolia												3						
	Sterculia tragacantha									1	1								
Ulmaceae	*Celtis zenkeri*											1							
Verbenaceae	*Vitex doniana*		1		1				1		1	1		6	2	1		1	
	Vitex grandifolia													2	4				

Table B1. Percentage and area of change images falling into each change class in the two comparisons, TM 1986 with ETM+ 2000 and ETM+ 2000 with ASTER 2006, with pixels that were burnt in either or both images masked out. The percentage significant positive change divided by the number of years of comparison is also included.

	1986–2000		2000–06	
Class	Percent	Area (km^2)	Percent	Area (km^2)
Significant positive change (>+2 std dev)	6.78	366.3	2.85	153.9
Marginally significant positive change (>+1 std dev)	8.08	436.4	4.05	218.5
No change (−1 to +1 std dev)	51.01	2754.6	65.24	3522.9
Marginally significant negative change (<−1 std dev)	3.7	200.2	0.69	37.7
Significant negative change (<−2 std dev)	0.22	12.3	0.41	22.3
Masked (burnt in at least one time point)	25.8	1393.4	16.98	917.1
Masked (water bodies and urban areas)	4.4	236.6	4.23	228.4
Masked (areas not present in 2006 mosaic)	N/A	N/A	5.54	299.2
Significant positive change per year (%)	0.48% yr^{-1}		0.47% yr^{-1}	

Appendix B

Additional Analysis with Fire Scars Removed

B.1. Methodology

A supervised spectral angle mapper classification was applied at each time point, using all available bands, and a training dataset of 25 areas chosen based on local field knowledge. It is impossible to assess the accuracy of these classifications, but they appeared consistent with our field knowledge, with the purple areas known to correspond to burn scars in 5–4–3 composites clearly picked out. The normalized image differencing technique was then applied as before, but with burnt areas as well as water bodies removed, and no thresholding of low NDVI values.

B.2. Results

The results are summarized Table B1 and Figure B1.

B.3. Discussion

While the areas and percentages increasing in both time points have been reduced by around half by this methodology, that is to be expected, as a large area of savanna has been removed from both comparisons. However, the areas of increase are still very significant (366 km^2 showing a significant increase from 1986 to 2000, 154 km^2 from 2000 to 2006), showing that the increases observed are not merely an artifact caused by the thresholding of low NDVI values as in the original analysis.

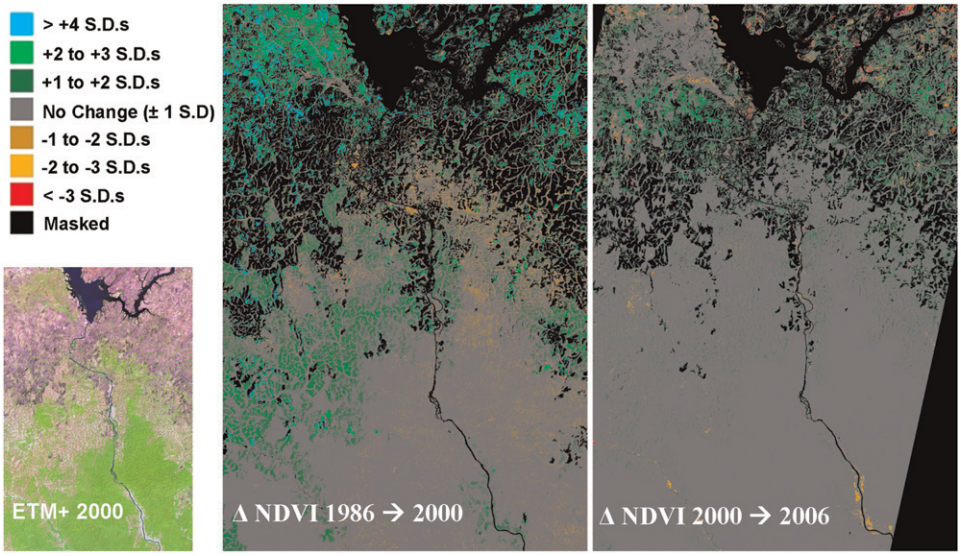

Figure B1. Two images showing the change in NDVI between 1986 and 2000 and 2000 and 2006, in standard deviations, with fire scars present at either time point in each comparison masked. Changes >±2 standard deviations should be considered significant at the 95% level. The 5–4–3 composite image from 2000 is also included.

The increase in percentage significant change per year observed using the original analysis has disappeared here, suggesting that this observed increase may not be significant. However, this is caused by a decrease in burnt area found in the 2006 images as compared to the 2000 image, which results in this technique removing a significant quantity of the positive change that occurred over this time period.

The analysis as presented in the paper is appropriate and robust; however, this analysis is considerably more conservative as it removes all burnt areas, following the methodology of, for example, Nangendo et al. (Nangendo et al. 2005). It should be viewed as supplementary verification that the observed results are not an artifact of the methodology.

References

Archer, S., T. W. Boutton, and K. A. Hibbard, 2001: Trees in grasslands: Biogeochemical consequences of woody plant expansion. *Global Biogeochemical Cycles in the Climate System,* E.-D. Schulze et al., Eds., Academic Press, 115–133.

Archibald, S., and R. J. Scholes, 2007: Leaf green-up in a semi-arid African savanna—Separating tree and grass responses to environmental cues. *J. Veg. Sci.,* **18,** 583–594.

Arino, O., S. Plummer, and D. Defrenne, 2005: Fire disturbance: The ten years time series of the ATSR world fire atlas. *Proc. MERIS (A)ATSR Workshop 2005,* Frascati, Italy, ESRIN, 30.1.

Bernstein, L., and Coauthors, 2007: *Climate Change 2007: Synthesis Report*. IPCC, Geneva, Switzerland, 104 pp.

Bond, W. J., and G. F. Midgley, 2000: A proposed CO_2-controlled mechanism of woody plant invasion in grasslands and savannas. *Global Change Biol.,* **6,** 865–869.

Boulvert, Y., 1990: Avancée ou recul de la forêt centroafricaine. Changements climatiques, influence de l'homme et notamment de feux. *Paysages Quaternaries de l'Afrique Central Atlantique,* R. Lanfranchi and D. Schwartz, Eds., Initiations et Didactiques, Orstrom, 353–366.

Bowman, D. M. J. S., A. Walsh, and D. J. Milne, 2001: Forest expansion and grassland contraction within a Eucalyptus savanna matrix between 1941 and 1994 at Litchfield National Park in the Australian monsoon tropics. *Global Ecol. Biogeogr.,* **10,** 535–548.

Brook, B. W., and D. Bowman, 2006: Postcards from the past: Charting the landscape-scale conversion of tropical Australian savanna to closed forest during the 20th century. *Landscape Ecol.,* **21,** 1253–1266.

Bucini, G., and N. P. Hanan, 2007: A continental-scale analysis of tree cover in African savannas. *Global Ecol. Biogeogr.,* **16,** 593–605.

Center for International Earth Science Information Network (CIESIN), cited 2004: Global Rural-Urban Mapping Project. (GRUMP): Urban/rural population grids. [Available online at http://sedac.ciesin.columbia.edu/gpw/.]

Chen, Z., C. D. Elvidge, and D. P. Groeneveld, 1998: Monitoring seasonal dynamics of arid land vegetation using AVIRIS data. *Remote Sens. Environ.,* **65,** 255–266.

Coppin, P., I. Jonckheere, K. Nackaerts, B. Mys, and E. Lambin, 2004: Digital change detection methods in ecosystem monitoring: A review. *Int. J. Remote Sens.,* **25,** 1565–1569.

Couteron, P., M. Deshayes, and C. Roches, 2001: A flexible approach for woody cover assessment from SPOT HRV XS data in semi-arid West Africa. Application in northern Burkina Faso. *Int. J. Remote Sens.,* **22,** 1029–1051.

Duarte, L. D. S., R. E. Machado, S. M. Hartz, and V. D. Pillar, 2006: What saplings can tell us about forest expansion over natural grasslands. *J. Veg. Sci.,* **17,** 799–808.

Durigan, G., and J. A. Ratter, 2006: Successional changes in cerrado and cerrado/forest ecotonal vegetation in western Sao Paulo State, Brazil, 1962–2000. *Edinburgh J. Bot.,* **63,** 119–130.

Eamus, D., and A. R. Palmer, 2007: Is climate change a possible explanation for woody thickening in arid and semi-arid regions? *Res. Lett. Ecol.,* **2007,** 37364, doi:10.1155/2007/37364.

Favier, C., J. Chave, A. Fabing, D. Schwartz, and M. A. Dubois, 2004: Modelling forest-savanna mosaic dynamics in man-influenced environments: Effects of fire, climate and soil heterogeneity. *Ecol. Modell.,* **171,** 85–102.

Felderhof, L., and D. Gillieson, 2006: Comparison of fire patterns and fire frequency in two tropical savanna bioregions. *Austral Ecol.,* **31,** 736–746.

Ferreira, L. G., and A. R. Huete, 2004: Assessing the seasonal dynamics of the Brazilian Cerrado vegetation through the use of spectral vegetation indices. *Int. J. Remote Sens.,* **25,** 1837–1860.

——, H. Yoshioka, A. Huete, and E. E. Sano, 2004: Optical characterization of the Brazilian savanna phyiognomies for improved land cover monitoring of the cerrado biome: Preliminary assessments from an airborne campaign over an LBA core site. *J. Arid Environ.,* **56,** 425–447.

Fuller, D. O., S. D. Prince, and W. L. Astle, 1997: The influence of canopy strata on remotely sensed observations of savanna-woodlands. *Int. J. Remote Sens.,* **18,** 2985–3009.

George, C., C. Rowland, F. Gerard, and H. Balzter, 2006: Retrospective mapping of burnt areas in Central Siberia using a modification of the normalised difference water index. *Remote Sens. Environ.,* **104,** 346–359.

Guillet, B., G. Achoundong, J. Y. Happi, V. K. K. Beyala, J. Bonvallot, B. Riera, A. Mariotti, and D. Schwartz, 2001: Agreement between floristic and soil organic carbon isotope ($^{13}C/^{12}C$, ^{14}C) indicators of forest invasion of savannas during the last century in Cameroon. *J. Trop. Ecol.,* **17,** 809–832.

Guyer, J. I., 2002: Briefing: The Chad-Cameroon petroleum and pipeline development project. *Afr. Aff.,* **101,** 109–115.

Happi, J. Y., 1998: *Arbres contre graminees: La lenta invasion de la savane par la foret au center-Cameroun*. Doctoral thesis, Université de Paris Sorbonne, 237 pp.

Hély, C., L. Bremond, S. Alleaume, B. Smith, M. T. Sykes, and J. Guiot, 2006: Sensitivity of African biomes to changes in precipitation regime. *Global Ecol. Biogeogr.,* **15,** 258–270.

Hopkins, M. S., J. Head, J. E. Ash, R. K. Hewett, and A. W. Graham, 1996: Evidence of a Holocene and continuing recent expansion of lowland rain forest in humid, tropical north Queensland. *J. Biogeogr.,* **6,** 737–745.

Huete, A., C. Justice, and H. Liu, 1994: Development of vegetation and soil indices for MODIS EOS. *Remote Sens. Environ.,* **49,** 224–234.

——, K. Didan, T. Miura, E. P. Rodriguez, X. Gao, and L. G. Ferreira, 2002: Overview of the radiometric and biophysical performance of the MODIS vegetation indices. *Remote Sens. Environ.,* **83,** 195–213.

Kummerow, C., and Coauthors, 2001: The evolution of the Goddard Profiling Algorithm (GPROF) for rainfall estimation from passive microwave sensors. *J. Appl. Meteor.,* **40,** 1801–1820.

Lambin, E. F., K. Goyvaerts, and C. Petit, 2003: Remotely-sensed indicators of burning efficiency of savannah and forest fires. *Int. J. Remote Sens.,* **24,** 3105–3118.

Leprieur, C., Y. H. Kerr, S. Mastorchio, and J. C. Meunier, 2000: Monitoring vegetation cover across semi-arid regions: Comparison of remote observations from various scales. *Int. J. Remote Sens.,* **21,** 281–300.

Lloyd, J., and G. D. Farquhar, 2008: Effects of rising temperatures and [CO_2] on the physiology of tropical forest trees. *Philos. Trans. Roy. Soc. London,* **B363,** 1811–1817.

Lu, D., 2006: The potential and challenge of remote sensing-based biomass estimation. *Int. J. Remote Sens.,* **27,** 1297–1328.

——, P. Mausel, E. Brondizio, and E. Moran, 2004: Change detection techniques. *Int. J. Remote Sens.,* **25,** 2365–2401.

Lu, H., M. R. Raupach, T. R. McVicar, and D. J. Barrett, 2003: Decomposition of vegetation cover into woody and herbaceous components using AVHRR NDVI time series. *Remote Sens. Environ.,* **86,** 1–18.

Maley, J., 1996: The African rain-forest—Main characteristics of changes in vegetation and climate from the Upper Cretaceous to the Quaternary. *Proc. Roy. Soc. Edinburgh,* **104,** 31–73.

Malhi, Y., and J. Wright, 2004: Spatial patterns and recent trends in the climate of tropical rainforest regions. *Philos. Trans. Roy. Soc. London,* **B359,** 311–329.

Marimon, B. S., E. S. Lima, T. G. Duarte, L. C. Chieregatto, and J. A. Ratter, 2006: Observations on the vegetation of northeastern Mato Grosso, Brazil. IV. An analysis of the cerrado-Amazonian forest ecotone. *Edinburgh J. Bot.,* **63,** 323–341.

Mayaux, P., E. Batholomé, S. Fritz, and A. Belward, 2004: A new land-cover map of Africa for the year 2000. *J. Biogeogr.,* **31,** 861–877.

Menaut, J. C., 1977: Evolution of plots protected from fire since 13 years in a Guinea savanna of Ivory Coast. *Actas IV Simposium Internacional Ecología Tropical,* Impresora Nación, LNAC, Panama, 541–481.

Ministère des Forêts et de la Faune, 2007: Parc National du Mbam et Djerem, Plan d'Aménagement 2007-2011. Republique du Cameroun, 137 pp. [Available online at http://archive.wcs.org/media/file/MbamDjeremMangementPlanDraft.pdf.]

Mitchell, T. D., and P. D. Jones, 2005: An improved method of constructing a database of monthly climate observations and associated high-resolution grids. *Int. J. Climatol.,* **25,** 693–712.

Nangendo, G., O. van Straaten, and A. de Gier, 2005: Biodiversity conservation through burning: A case study of woodlands in Budongo Forest Reserve, NW Uganda. *African Forests between Nature and Livelihood Resources: Interdisciplinary Studies in Conservation and Forest Management,* M. A. F. Ros-Tonen and T. Dietz, Eds., Edwin Mellen, 113–128.

Pettorelli, N., J. O. Vik, A. Mysterud, J. M. Gaillard, C. J. Tucker, and N. C. Stenseth, 2005: Using the satellite-derived NDVI to assess ecological responses to environmental change. *Trends Ecol. Evol.,* **20,** 503–510.

Pinzon, J., M. E. Brown, and C. J. Tucker, 2005: Satellite time series correction of orbital drift artifacts using empirical mode decomposition. *Hilbert-Huang Transform: Introduction and Applications,* N. Huang, Ed., World Scientific, 167–186.

Polley, H. W., H. S. Mayeux, H. B. Johnson, and C. R. Tischler, 1997: Viewpoint: Atmospheric CO_2, soil water and shrub/grass ratios on rangelands. *J. Range Manage.,* **50,** 278–284.

Puyravaud, J. P., C. Dufour, and S. Aravajy, 2003: Rain forest expansion mediated by successional processes in vegetation thickets in the Western Ghats of India. *J. Biogeogr.,* **30,** 1067–1080.

Qi, J., A. Chehbouni, A. R. Huete, and Y. H. Kerr, 1994: A modified soil adjusted vegetation index. *Remote Sens. Environ.,* **48,** 119–126.

Qin, W., and S. A. W. Gerstl, 2000: 3-D Scene modeling of semidesert vegetation cover and its radiation regime. *Remote Sens. Environ.,* **74,** 145–162.

Roitman, I., J. M. Felfili, and A. V. Rezende, 2008: Tree dynamics of a fire-protected *cerrado sensu stricto* surrounded by forest plantation, over a 13-year period (1991-2004) in Bahia, Brazil. *Plant Ecol.,* **197,** 255–267.

Russell-Smith, J., P. J. Stanton, A. C. Edwards, and P. J. Whitehead, 2004: Rain forest invasion of eucalypt-dominated woodland savanna, Iron Range, north-eastern Australia: II. Rates of landscape change. *J. Biogeogr.,* **31,** 1305–1316.

Salzmann, U., and P. Hoelzmann, 2005: The Dahomey Gap: An abrupt climatically induced rain forest fragmentation in West Africa during the late Holocene. *Holocene,* **15,** 190–199.

Sankaran, M., and Coauthors, 2005: Determinants of woody cover in African savannas. *Nature,* **438,** 846–849.

Sedano, F., P. Gong, and M. Ferrao, 2005: Land cover assessment with MODIS imagery in southern African Miombo ecosystems. *Remote Sens. Environ.,* **98,** 429–441.

Singh, A., 1989: Review article: Digital change detection techniques using remotely-sensed data. *Int. J. Remote Sens.,* **10,** 989–1003.

Songh, C., C. E. Woodcock, K. C. Seto, M. P. Lenney, and S. A. Macomber, 2001: Classification and change detection using Landsat TM data: When and how to correct atmospheric effects? *Remote Sens. Environ.,* **75,** 230–244.

Su, L., M. J. Chopping, A. Rango, J. V. Martonchik, and D. P. C. Peters, 2007: Support vector machines for recognition of semi-arid vegetation types using MISR multi-angle imagery. *Remote Sens. Environ.,* **107,** 299–311.

Swaine, M. D., W. D. Hawthorne, and T. K. Orgle, 1992: The effects of fire exclusion on savanna vegetation at Kpong, Ghana. *Biotropica,* **24,** 166–172.

Tucker, C. J., J. E. Pinzon, M. E. Brown, D. Slayback, E. W. Pak, R. Mahoney, E. Vermote, and N. El Saleous, 2005: An extended AVHRR 8-km NDVI data set compatible with MODIS and SPOT vegetation NDVI data. *Int. J. Remote Sens.,* **26,** 4485–4498.

Vauttoux, R., 1976: Contribution a l'etude de l'evolution des strates arboree et arbustive dans la savane de Lamto (Cote-d'Ivore). *Ann. Univ. Abidjan,* **13,** 35–63.

World Bank, cited 2007: World Bank Development Indicators Database. World Bank, Washington DC. [Available online at http://www.worldbank.org/data/onlinedatabases/wdi.]

Xiao, J., and A. Moody, 2005: A comparison of methods for estimating fractional green vegetation cover within a desert-to-upland transition zone in central New Mexico, USA. *Remote Sens. Environ.,* **98,** 237–250.

Zeng, N., and D. Neelin, 2000: The role of vegetation–climate interaction and interannual variability in shaping the African savanna. *J. Climate,* **13,** 2665–2670.